As per UGC guidelines an electronic bar code is provided to seure your paper

International Journal for Modern Trends in Science and Technology, 8(02): 75-86, 2022

ISSN: 2455-3778 online
DOI: https://doi.org/10.46501/IJMTST0802013
Available online at: http://www.ijmtst.com/vol8issue02.html

A comparison on Energy Dissipation Mechanism of SPO Analysis and NLTHA for 44 Story RC Building

Mistreselasie S. Abate[1*] | Vivian W.Y. Tam[2] | Ana Catariana Jorge Evangelista[3] | Seble-W Kassa[4]

[1*]Departmentof Civil and Structural, Engineering Institute of Technology, Perth, Australia, 12536@student.eit.edu.au
[2]Western Sydney University, School of Engineering, Design and Built Environment, Locked Bag 1797, Penrith, NSW 2751, Australia, v.tam@westernsydney.edu.aul
[3]Departmentof Civil and Structural,Engineering Institute of Technology, Perth, Australia, Ana.evangelista@eit.edu.au
[4]Departmentof Science, Engineering and Computing, Kingston University, London, UK. seble_wk2016@yahoo.com

To Cite this Article
Mistreselasie S. Abate, Vivian W.Y. Tam, Ana Catariana Jorge Evangelista and Seble-W Kassa. A comparison on Energy Dissipation Mechanism of SPO Analysis and NLTHA for 44 Story RC Building. *International Journal for Modern Trends in Science and Technology* 2022, *8* pp. 75-86. https://doi.org/10.46501/IJMTST0802013

Article Info
Received: 02 January 2022; Accepted: 28 January 2022; Published: 05 February 2022.

ABSTRACT

The seismic performance of RC structure 3D-models analyzed according to Ethiopian ES8-15 corresponds to Eurocode 8-2004 standards (based on EN1998-1) seismic code recommendations is presented. In this study, sample nonlinear models 44 story was used. RC building was analyzed by Static Dynamic analysis (SPO) and NLTHA with selected 11 ground motions from PEER website with ETABS vs. 19.0.0 software. To match the selected ground motions with target response spectrum as per ES8-15 elastic spectrum type I, both Seismo-match and ETABS vs. 19.0.0 software were used. The objective of this study is to present the energy dissipation mechanism of the two analysis types. How much of the energy of the applied loading dissipated by which component of the structure? The nonlinear static (pushover) methodologies of FEMA 356, ASCE 41-17 and ATC 40 requirements are then used to assess their seismic performance. DNLTHA was used to validate the analysis results. kinematics, potential, Global Damping, Nonlinear Vicious Damping, Non-linear hysteresis Damping quantities toward the energy dissipation of the building are among the comparison parameters. The results show that the structures' energy dissipation mechanism is hugely different for the two analysis types. Finally, the study demonstrated the positive elements of both analyses, which will be useful in future research.

KEYWORDS:Global Damping, kinematics, Nonlinear Vicious Damping, Non-linear hysteresis Damping, potential

1. INTRODUCTION

Seismic response is often evaluated in practical design applications using linear elastic structure behavior. However, this strategy may be ineffective in limiting the extent of structure damage. To do this, more precise techniques of analysis are necessary that can accurately forecast the true behavior of structures subjected to significant seismic forces. The most rigorous technique is non-linear dynamic analysis, although it is still too difficult for design usage. The non-linear static pushover analysis seems to be a more sensible approach for determining the lateral strength and distribution of inelastic deformations. Several simpler non-linear approaches have been developed in recent years [1]. were designed in order to forecast seismic demand using pushover analysis data. These

techniques have also been included into contemporary recommendations [2],[3] which are based on performance-based engineering ideas. The pushover analysis was used in this study to determine the reaction of an RC construction. Pushover studies with various load distributions and incremental dynamic assessments with a large number of seismic movements were conducted. The goal of this study was to compare NL static& dynamic analytic approaches. The assessment of seismic demand was previously conducted using well-known simplified approaches such as the N2 and capacity spectrum method. The purpose of this research was to compare the different methodologies and their results to dynamic evaluations of the structure's energy dissipation process [4].

RESEARCH QUESTION

How much of the energy of the applied loading dissipated by which component of the structure?

RELEVANCE AND IMPORTANCE OF THE RESEARC

This study endeavors to further our knowledge of the seismic design issues that extremely tall structures encounter, as well as their structural design. Additionally, it would help in the assessment of building energy dissipation principles and seismic ground motion characteristics at the component level. Elastic analysis methodologies do not take into account the redistribution of seismic demand among the building's different components during periods of inelastic activity.

RESEARCH OBJECTIVE

The research will analyze the potential benefits of lessons learnt from high-rise building seismic design challenges in terms of the structure's energy dissipation mechanism for SPO and NLTHA methods. Additionally, develop a policy that is specific to each technology advancement, such as PBD. Specifically, the strategic elements that should be incorporated into the design of tall buildings in e-government policies and as a guideline for Ethiopia's local consulting and design companies, as well as internationally, by focusing on the energy dissipation of various high-rise buildings.

2. LITRATURE REVIEW

If the ductility is more than 3, it is feasible to get a FEMA-440 grade equivalent to damping. This damping is determined by summing the hysteretic energy lost by all of the design's plastic hinges [5]. Corrosion's adverse effects on the mechanical characteristics of steel and concrete may now be described using a systematic method. Corrosion has an effect on the failure mode sequence, flexural strength, and capacity of energy dissipation of RC building. Corrosion penetration increases with depth, accumulating damage mostly in constrained concrete [6]. For earthquake design, the inner stability of RC earth retaining walls is crucial. The seismic behavior of earth retaining walls was investigated using a discretization technique and the (UBT), the theorem of upper bound for limit analysis [7]. The University of Bristol's Journal of Electrochemistry and Bio macromolecular Engineering demonstrates that FRP composites may be used as internal reinforcement in RC beam-column connections that have been broken (JEC-BME)[8],[9].Aberystwyth University researchers used fiber-reinforced polymer (FRP) composite internal reinforcement to repair sulfate-damaged RC beam-column connections. The capacity of a joint to withstand rotation and bearing loads is crucial in earthquake-prone locations. Plate reinforced connections effectively prevent beam-end welds from brittle failure. Due to the findings of this research [10], high-strength steel joints may now be used and supplied widely in the engineering business. By using this material, RC structures may benefit from an improvement in their energy dissipation capabilities. The seismic performance of RC structures reinforced using a variety of high-strength rubberized concrete mixtures is investigated under a variety of ground movements. Rubberized concrete was found to be an excellent material for rebuilding RC structures by enhancing damping energy and lowering the structure's base shear pressures [11]. Composite structures made of steel and steel fiber RC (SSFRC) have been dubbed "revolutionary" due to its new design.4-point bending tests were performed on a total of 18 SSFRC beams with various shear span ratios, steel fiber volume fractions, and shaped steel ratios. Increased bending steel in a structure may significantly enhance energy dissipation [12]. Corrosive conditions have shortened the life of existing reinforced concrete buildings and reduced their seismic performance. At two different levels of typical column axial force ratio, eight RC external joints with variable degrees of corrosion protection were exposed to the test. Inthe link between joint shear stress and

longitudinal reinforcement development was investigated [13].

3. GAP IN THE EXISTING KNOWLEDGE

According to recent research PBD is a modern EQ design approach which is widely used to examine the seismic performance of already built buildings & to design a number of new tall structures. According to an extensive review of the literature, considerable work has been done on the energy dissipation of applied loading on various structures using a variety of different approaches; however, to our knowledge, none of them examined the structure's energy dissipation mechanism in terms of kinematics, potential, global damping, nonlinear vicious damping, and nonlinear hysteresis damping. Thus, the purpose of this study is to address the research issue, "How much energy is wasted by which component of the structure?" For the SPO and NLTHA of a 44-story example RCbuilding.

4. RESEARCH METHODS

The study will look at the benefits of using lessons learned from high-rise building EQ design issues. In this case, the study will look at how the structure's energy dissipation mechanism works for SPO and NLTHA approaches. Another thing you can do is make a policy that fits the progress of each technology, like PBSD. The strategic elements that should be used in the design of tall buildings in Ethiopia's e-government policies and as a guide for Ethiopian consulting and construction firms, as well as those that work outside of Ethiopia, are focused on the energy dissipation of different high-rise buildings. compare the results of SPO and NLTHA seismic design to those produced by PBD method. In particular, the researchers want to look at the structure's energy dissipation mechanism in terms of how it responds to a given load. To show and compare the performance of a few hinges that were made specifically with SPO and NLTHA.

Method and source;

The EQ resilience performance of RC buildings 3D-models designed in compliance to Ethiopian ES8-15 corresponds to Eurocode 8-2004 standards (based on EN1998-1) seismic code recommendations is presented. In this study, sample nonlinear models 44 story was used. RC building was analyzed by Static Dynamic analysis (SPO) and NLTHA with selected 11 ground motions from PEER website with ETABS vs. 19.0.0 software. To match the selected ground motions with target response spectrum as per ES8-15 elastic spectrum type I, both Seismo-match and ETABS vs. 19.0.0 software were used. The objective of this study is to present the energy dissipation mechanism of the two analysis types. How much of the energy of the applied loading dissipated by which component of the structure? The nonlinear static (pushover) methodologies of FEMA 356, ASCE 41-17 and ATC 40 requirements are then used to assess their seismic performance.

5. MODELING AND ANALYSIS IN ETABS

Multi-story building analysis and design is made possible by ETABS, a computer software tool. All modeling tools and templates, as well as load prescriptions, analysis techniques, and solution strategies based on code, are aligned with the grid-like geometry that is unique to this kind of construction in order to take use of it. In accordance with the scenario, ETABS may be used to study simple or complex systems in either a static or dynamic context. The utilization of modal and direct integration THA studies in conjunction with P-Delta and the effect of Large Displacement, as well as other seismic performance assessment techniques, may be employed to offer a thorough evaluation of seismic performance. When nonlinear connections, concentrated PMM, or fiber hinges exhibit monotonic or hysteretic behavior, it is possible that they will be able to catch material nonlinearity and capture it successfully. With the help of straightforward and integrated functionality, developers may create apps of any complexity level. When used in conjunction with ETABS, a wide variety of design and documentation platforms are compatible, making it feasible to coordinate and develop designs ranging from simple two-dimensional frames to complicated modern high-rise structures.

Building Detail;

The current research examines a G+44 building with a floor height of three and a soil type of medium soil (type B) in Zone III. M30-concrete is used for the beams and slabs, while M30-concrete is used for the columns. Fe-460 steel is used for the columns. According to ES8-15, conforms to Eurocode 8-2004 requirements (based on EN1998-1) - The damping ratio used five percent, the zone factor (Z) is fixed to 0.36, and the importance factor (I) is fixed to 1m. The live load of 3 kN/m2 (as specified in ES8-15) is equivalent to

Eurocode 8-2004 requirements (based on EN1998-1). 1.5 kN/m2 for the floor finish the measurements of the members,materialproperty,sectionproperty,and slab properites are listed in Table 1-3. The target response spectrum and the mean time history datas are shown in **Figure no. 5-11** and Table 4.

Table 1- Material Property - General

Material Properties - General				
Material	**Type**	**SymType**	**Grade**	**Color**
4000Psi	Concrete	Isotropic	f'c 4000 psi	Gray8Dark
A416Gr270	Tendon	Uniaxial	Grade 270	Green
A615Gr60	Rebar	Uniaxial	Grade 60	Blue
A992Fy50	Steel	Isotropic	Grade 50	Yellow

Table 2- Frame Section Property Definitions-ConcretRectangular

Frame Section Property Definitions - Concrete Rectangular					
Name	**Material**	**From File?**	**Depth**	**Width**	**Rigid Zone?**
			mm	mm	
ConcBm	4000Psi	No	700	500	No
ConcCol	4000Psi	No	1000	700	No

Table 3- Area Section Property Definitions -Summary

Area Section Property Definitions - Summary						
Name	**Type**	**Element Type**	**Material**	**Total Thickness**	**Deck Material**	**Deck Depth**
				mm		mm
Deck1	Deck	Membrane	4000Psi	162.5	A992Fy50	75
Plank1	Slab	Membrane	4000Psi	200		
Slab1	Slab	Shell-Th	4000Ps	150		
		in	i			
Wall1	Wall	Shell-Thin	4000Psi	500		

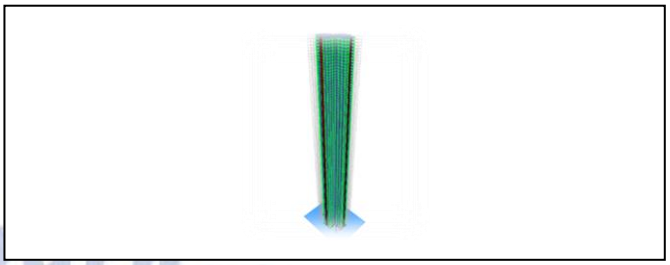

Figure no 1: Sample 44 Story Linear 3-D Modelling

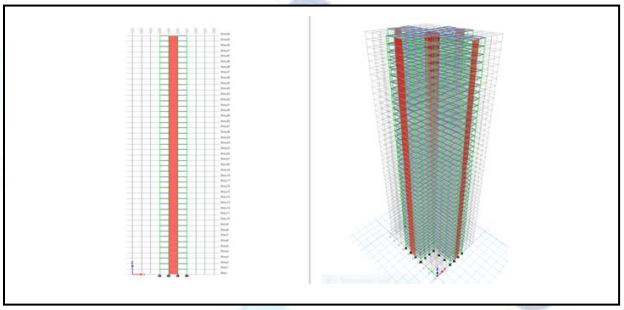

Figure no 2- Elevation and 3D view of 44 story sample Linear building

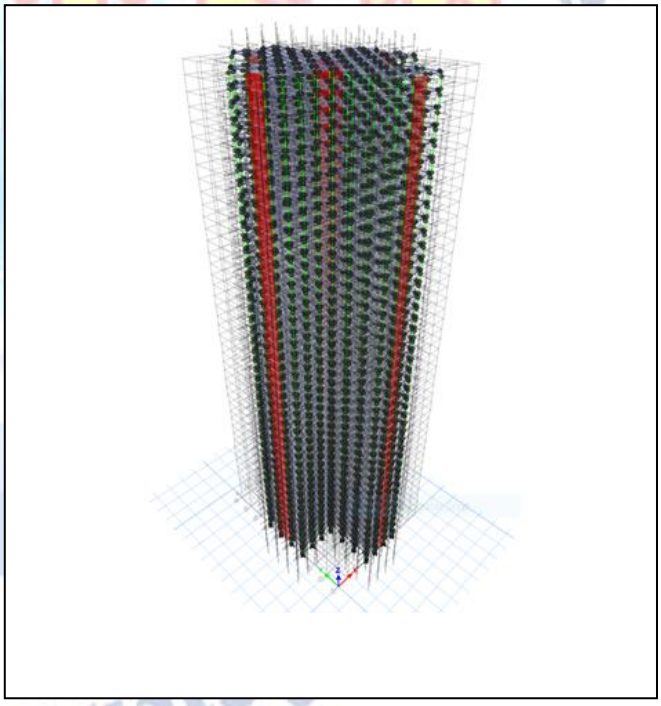

Figure no 3:3D Model of Non-Linear Modelling Plastic Hinge Modelling Approach

Model of RC frame;

This section gives a quick overview of how the model structure in the study were designed utilizing Ethiopian building codes ES8-15 adhere Eurocode 8-2004 regulations. Following that, the design results will be

utilized to test the models' seismic performance in the subsequent Section. The material strength, loading, and geometry models in the two-example analysis were kept substantially identical to assess the design approaches and seismic provisions.

Model geometry, material strength, and gravitational load;

A typical structural design, as shown in **Figure no.2**, of a residential high-rise structure with an arrangement of 45mx36m and frames in the X-Y axis was used in this study to create the analytic model of buildings as shown in Table 3 and **Figure no.1-4**.

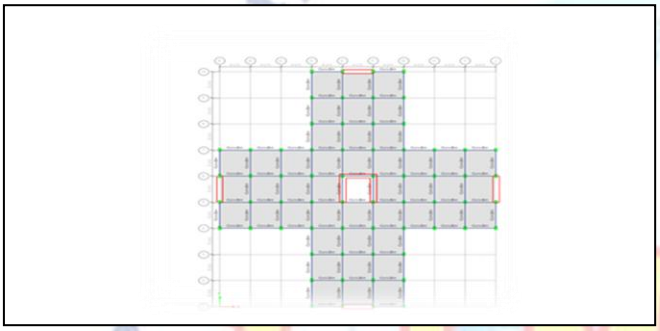

Figure no 4:A residential high-rise building with a plan layout of 45mx 36m and central model frames in the transverse direction

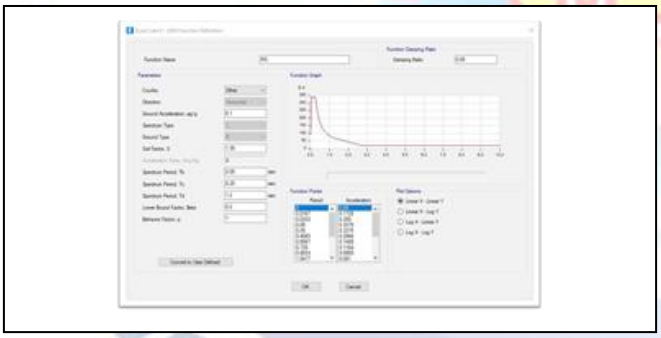

Figure no 5: ESB-2015-elastic spectra soil B 10% in 50 years

Figure no 6: ES8-15 adheres to Eurocode 8-2004 regulations design spectra soil B, q=5.85, 10% in 50 years

Table 4-Time History Date from PEER Website.

No	EQ	Year	Recording Station No.(RSN)	Mag	Vs30(m/s)	PGA(g)	Mechanism	Spectral Ordinate
1	"Imperial Valley-06"-US	1979	164	6.53	471.53	0.21	strike slip	SRSS
2	"Landers"-US	1992	881	7.28	396.41	0.21	strike slip	SRSS
3	"Mammoth Lakes-01"-US	1980	230	6.06	382.12	0.42	Normal Oblique	SRSS
4	"Landers"-US	1992	3757	7.28	367.84	0.13	strike slip	SRSS
5	"Loma Prieta"-US	1989	802	6.93	380.89	0.51	Reverse Oblique	SRSS
6	"Landers"-US	1992	3759	7.28	425.02	0.12	strike slip	SRSS
7	"Landers"-US	1992	832	7.28	382.93	0.089	strike slip	SRSS
8	"Chuetsu-oki_Japan"	2007	5274	6.8	430.71	0.13	Reverse	SRSS
9	"Northridge-01"-US	1994	1004	6.69	380.06	0.75	Reverse	SRSS
10	"Chi-Chi_Taiwan"	1999	1513	7.62	363.99	0.59	Reverse Oblique	SRSS
11	"Parkfield-02_CA"	2004	4070	6	378.99	0.62	strike slip	SRSS

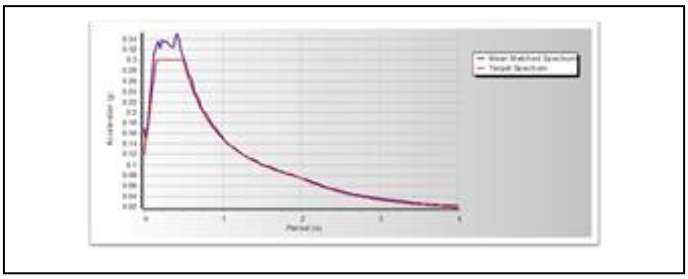

Figure no. 7: Mean Matched Spectrum for 11 Selected Ground Accelerations and Target Spectrum as per ES EN 1998-15

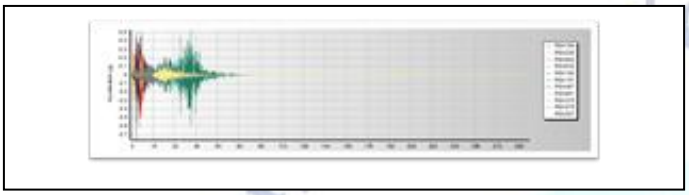

Figure no. 8: Seism match Representation of Eleven Ground Motions

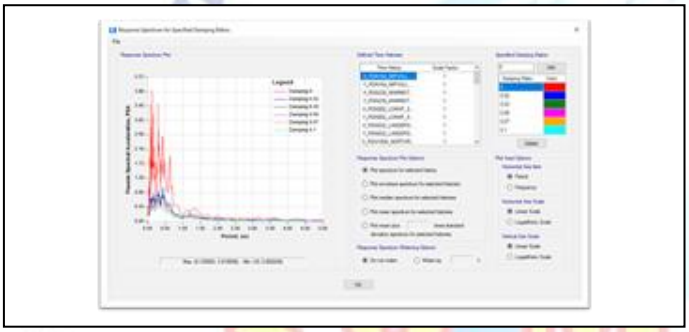

Figure no. 9:ETABS vs 19.0.0 Representation of Response Spectrum for Specified Damping Ratio X_RSN164 _IMPVALLY EQ

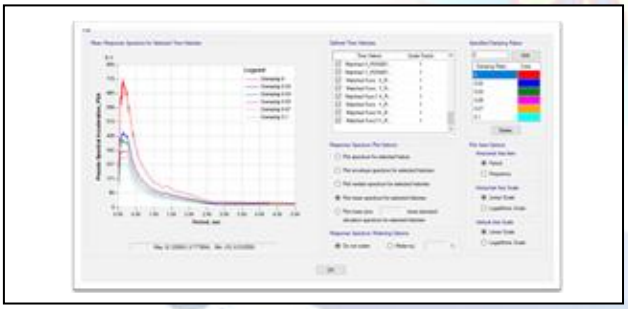

Figure no. 10: ETABS vs 19.0.0 Representation of Mean Response Spectrum for Specified Damping Ratio for sample Eleven Ground Motions

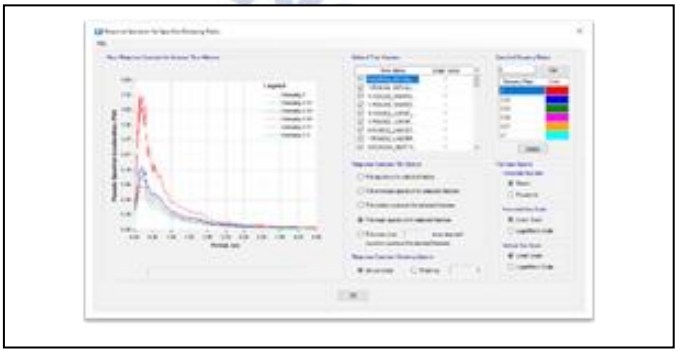

Figure no. 11: Response Spectrum for Specified Damping Rations and Mean spectrum for selected histories

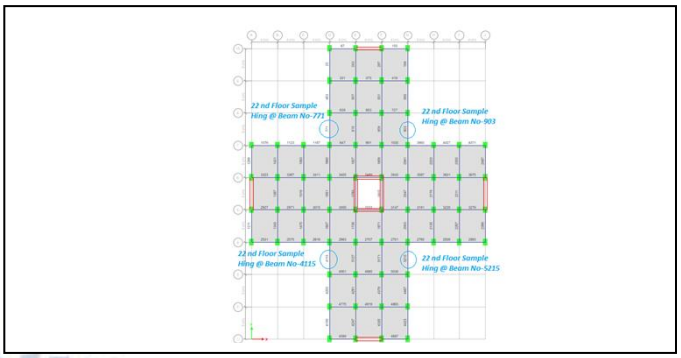

Figure no 12: SPO & NLTHA Sample Hing locations for Comparison

6. SPO ANALYSIS RESULT

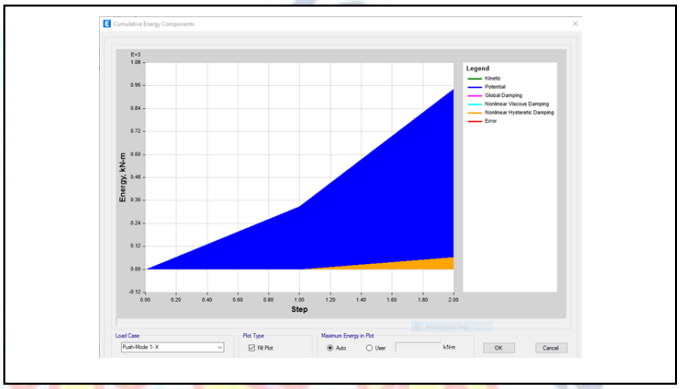

Figure no 13: Cumulative Energy Component as per Push-Mode 1-x load Case Result

1.From static pushover analysis cumulative energy component, it has been observed that energy dissipation of the applied force is mostly handled by potential part of the structure **(Figure no.13).**

2. From the analysis it has been observed that the non-linear hysteresis damping has small contribution toward the energy dissipation mechanism of the structure**(Figure13 no.13).**

3. From the analysis it has been observed that kinetic, Global Damping, Nonlinear global Damping and error in the structure has zero contribution toward the energy dissipations mechanism of the structure **(Figure13 no.13).**

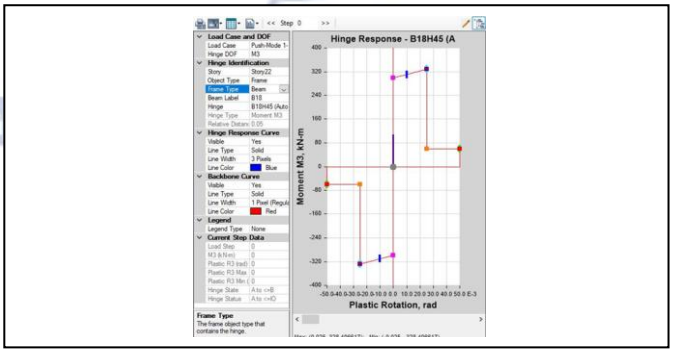

Figure no. 14: Hinge Response - B18H45 (Auto M3)-77

Table 5- Hing Response-- B18H45 (AUTO M3)-771

Hinge Response - B18H45 (Auto M3)-771						
Step	**M3**	**R3**	**R3 Max**	**R3 Min**	**State**	**Status**
	kN-m	rad	rad	rad		
0	0	0	0	0	A to <=B	A to <=IO
1	65.5997	0	0	0	A to <=B	A to <=IO
2	109.2087	0	0	0	A to <=B	A to <=IO

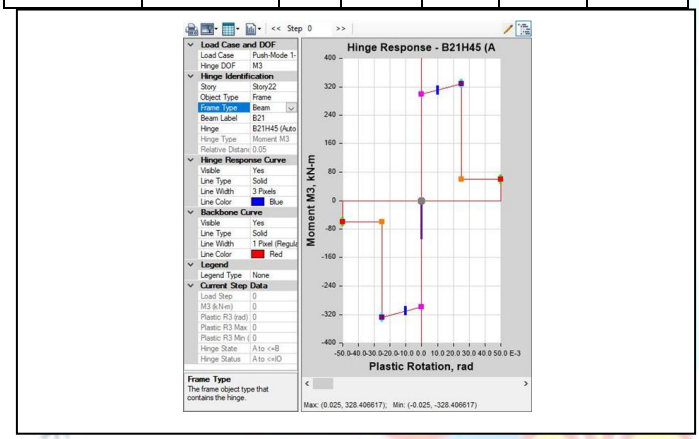

Figure no. 15: Hinge Response - B21H45 (Auto M3)-903

Table 6- HINGE RESPONSE - B21H45 (AUTO M3)-903

TABLE: Hinge Response - B21H45 (Auto M3)-903						
Step	**M3**	**R3**	**R3 Max**	**R3 Min**	**State**	**Status**
	kN-m	rad	rad	rad		
0	0	0	0	0	A to <=B	A to <=IO
1	-65.5952	0	0	0	A to <=B	A to <=IO
2	-109.226	0	0	0	A to <=B	A to <=IO

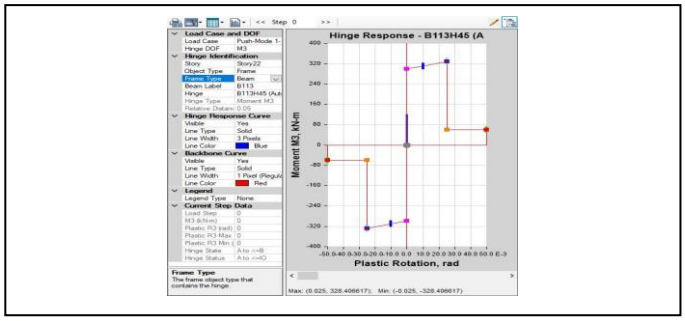

Figure no. 16- Hinge Response - B113H45 (Auto M3)-5215

Table 7- HINGE RESPONSE - B113H45 (AUTO M3)-5215

Hinge Response - B113H45 (Auto M3)-5215						
Step	**M3**	**R3**	**R3 Max**	**R3 Min**	**State**	**Status**
	kN-m	rad	rad	rad		
0	0	0	0	0	A to <=B	A to <=IO
1	72.3479	0	0	0	A to <=B	A to <=IO
2	119.991	0	0	0	A to <=B	A to <=IO

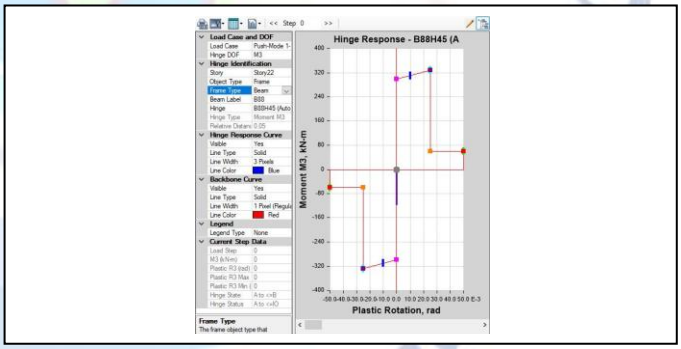

Figure no 17: Hinge Response - B88H45 (Auto M3)-4115

Table 8- HINGE RESPONSE - B88H45 (AUTO M3)-4115

Hinge Response - B88H45 (Auto M3)-4115						
Step	**M3**	**R3**	**R3 Max**	**R3 Min**	**State**	**Status**
	kN-m	rad	rad	rad		
0	0	0	0	0	A to <=B	A to <=IO
1	-72.3419	0	0	0	A to	A to

					<=B	<=IO
2	-119.2448	0	0	0	A to <=B	A to <=IO

In the nonlinear mode M-3 plastic hinges were assigned for beam in the nonlinearization of the modeling process and sample 4 beams were selected at 22nd floor and studied the behavior the hinges. The position of the hinges is shown in **Figure no. 12**. The SPO analysis result in **Figure no.13-14** and Table 6 shows that Hinge Response for hinge type B18H45 (Auto M3) was 65.6599 kn-m and 109.106 kn-m for step 1 and 2 respectively. Similarly, **Figure no.15** and Table 6 shows Hinge Response - B21H45 (Auto M3) with 65.5952 kn-m and 109.103 Kn-m respectively. In the same way for sample hinge type in **Figure no.16** and Table7 shows Hinge Response - B113H45 (Auto M3)- 72.3479 Kn-m and 119.991 KN-m for step 1 and 2 respectively. Finally, **Figure no.17** and Table 8 shows Hinge Response - B88H45 (Auto M3)-result of 72.3419 Kn-m and 119.2448 Kn-m for analysis step 1 and 2 respectively.

NONLINEAR NLRTHA DYNAMIC MODELING RESULT

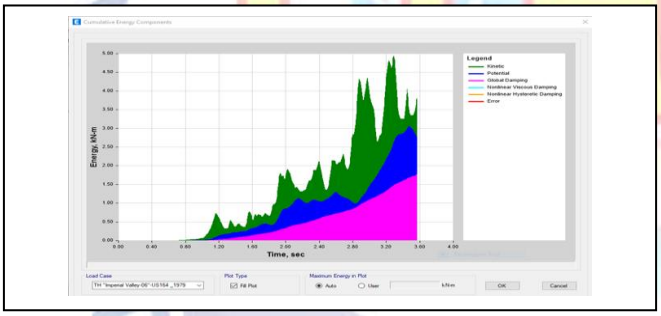

Figure no. 18: Cumulative Energy Component for NLDTH Analysis

1. From NLTHA analysis cumulative energy component, it has been observed that energy dissipation of the applied force is mostly handled by kinetic and Global damping part of the structure **(Figure no.18).**

2. From the analysis it was observed that the static part of the structure has significant contribution toward the energy dissipation mechanism of the structure **(Figure no.18).**

3. From the analysis it has been observed that Nonlinear Viscous damping, Nonlinear Hysteretic Damping, and error in the structure has zero contribution toward the energy dissipations mechanism of the structure **(Figure no.18).**

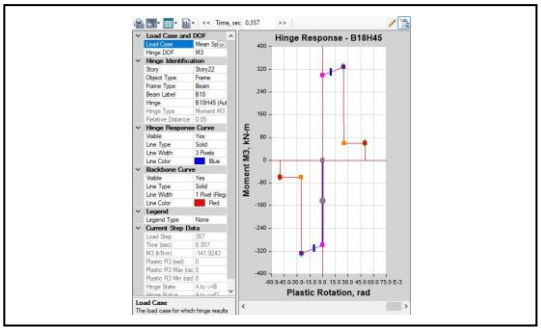

Figure no. 19- Hinge Response - B18H45 (Auto M3)-NLTHA-771

Table 9- HINGE RESPONSE - B18H45 (AUTO M3)-NLTHA-771

Hinge Response - B18H45 (Auto M3)-NLTHA-771						
Step	**M3**	**R3**	**R3 Max**	**R3 Min**	**State**	**Status**
	kN-m	rad	rad	rad		
0	0	0	0	0	A to <=B	A to <=IO
313	-66.0876	0	0	0	A to <=B	A to <=IO
1239	-300.1	0	0	0	B to <=C	A to <=IO

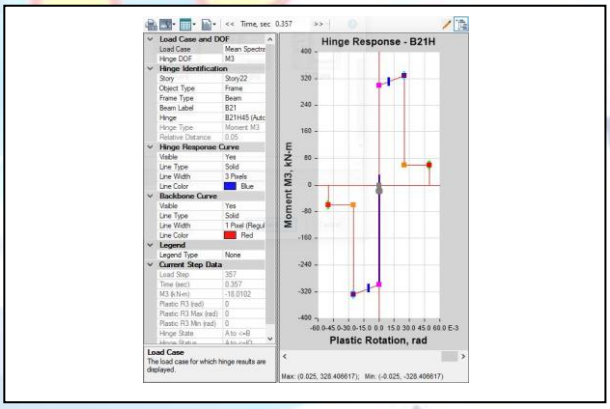

Figure no. 20: NLTHA Hinge Response - B21H45 (Auto M3)-903

Table 10- NLTHA HINGE RESPONSE - B21H45 (AUTO M3)-903

Hinge Response - B21H45 (Auto M3)-903						
Step	**M3**	**R3**	**R3 Max**	**R3 Min**	**State**	**Status**
	kN-m	rad	rad	rad		
0	0	0	0	0	A to <=B	A to <=IO

412	-65.3652	0	0	0	A to <=B	A to <=IO
1239	-299.2	0	0	0	B to <=C	A to <=IO

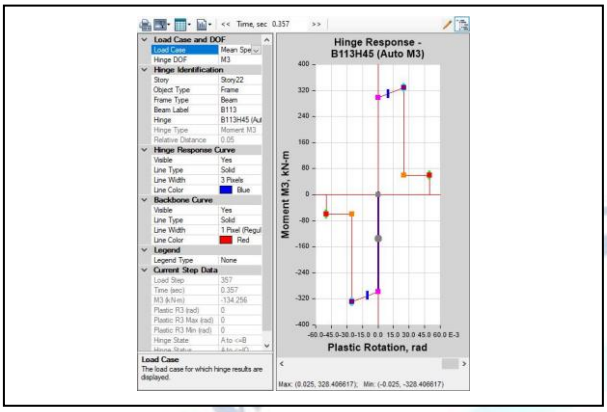

Figure no. 21- NLTHA Hinge Response - B113H45 (Auto M3)-5215

Table 11- NLTHA HINGE RESPONSE - B113H45 (AUTO M3)-5215

Hinge Response - B113H45 (Auto M3)-5215						
Step	**M3**	**R3**	**R3 Max**	**R3 Min**	**State**	**Status**
	kN-m	rad	rad	rad		
0	0	0	0	0	A to <=B	A to <=IO
321	72.0848	0	0	0	A to <=B	A to <=IO
1239	300.1	0	0	0	A to <=B	A to <=IO

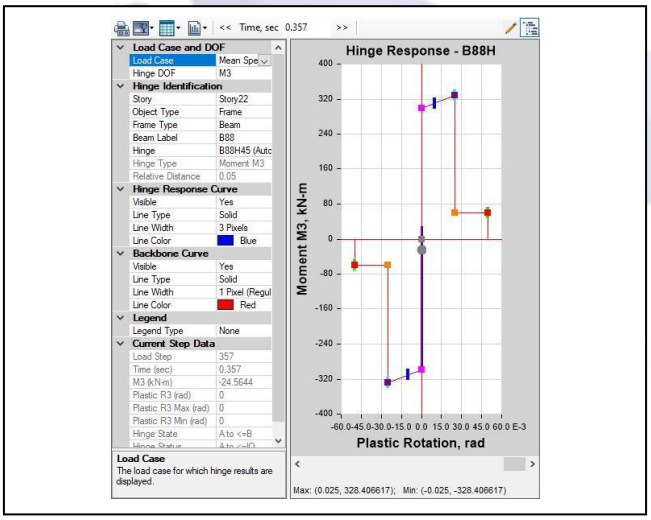

Figure no. 22: NLTHA Hinge Response - B88H45 (Auto M3)-4115.

Table 12- NLTHA HINGE RESPONSE - B88H45 (AUTO M3)-4115

Hinge Response - B88H45 (Auto M3)-4115						
Step	**M3**	**R3**	**R3 Max**	**R3 Min**	**State**	**Status**
	kN-m	rad	rad	rad		
0	0	0	0	0	A to <=B	A to <=IO
410	-72.676	0	0	0	A to <=B	A to <=IO
1239	299.2	0	0	0	B to <=C	A to <=IO

The NLTHA analysis result in **Figure no.18-19** and Table 9 shows that Hinge Response for hinge type B18H45 (Auto M3) was 66.0876 Kn-m and 300.1kn-m for step 321 and 1239 respectively. Similarly, **Figure no.20** and Table 10 shows Hinge Response - B21H45 (Auto M3) with 65.3652 KN-m and 299.1 Kn-m at analysis steps of 412 and 1239 respectively. In the same way for sample hinge type in **Figure no .21** and Table 11 shows Hinge Response - B113H45 (Auto M3)- 72.0848 Kn-m and 300.1 KN-m for step 321 and 1239 respectively. Finally, **Figrr no. 22** and Table12 shows Hinge Response - B88H45 (Auto M3)-result of 72.676 Kn-m and 299.2 Kn-m for analysis step 410 and 1239 respectively. Table 13 presents the summary of result of both analyses.

Table 13- Summary of SPO & NLTHA Analysis Hing Results

SPO Analysis Hing Results F-D curve					NLTHA hinge Results F-D Curves							
No	Hinge Response - B18H45 (Auto M3)-771	Hinge Response - B21H45 (Auto M3)-903	Hinge Response - B113H45 (Auto M3)-5215	Hinge Response - B88H45 (Auto M3)-4115	No	Hinge Response - B18H45 (Auto M3)-771	No	Hinge Response - B21H45 (Auto M3)	No	Hinge Response - B113H45 (Auto M3)-5215	No	Hinge Response - B88H45 (Auto M3)-4115
Step	M3 (KN-m)	M3(KN-m)	M3(KN-m)	M3(KN-m)	Step		Step		Step		Step	
0	0	0	0	0	0	0	0	0	0	0	0	0
1	65.5997	65.5952	72.3479	-72.3419	313	66.0876	412	65.3652	321	72.0848	410	72.676
2	109.2087	109.226	119.991	119.2448	1239	-300.1	1239	299.2	1239	300.1	1239	299.2

7. DISCUSSION

The most rigorous technique is the non-linear dynamic analysis, although it is still too complicated to be used in the design. The pushover analysis was used to investigate the reaction of an RC building in this study. Pushover studies with various load distributions were done, and incremental dynamic simulations.

RC 3D-models created following Ethiopian ES8-15 standards (based on EN1998-1) seismic code guidelines have seismic performance that is equivalent to that of Eurocode 8-2004-compliant reinforced concrete (RC) structures (based on EN1998-1). This study used non-linear sample models comprising 44 stories to analyze the data. A total of 11 ground movements were picked from the PEER website and used to analyze the RC building utilizing ETABS vs. 19.0.0 software and Dynamic Static Analysis (SPO) and NLTHA with the RC building. In order to match the chosen ground movements with the target response spectrum according to the ES8-15 elastic spectrum type I, the program Seismo-match and the ETABS vs. 19.0.0 were used.

From static pushover analysis cumulative energy component, it has been observed that energy dissipation of the applied force is mainly handled by potential part of the structure. It has been observed that the non-linear hysteresis damping has a small contribution toward the energy dissipation mechanism of the structure. Kinetic, Global Damping, Non-linear global Damping, and error in the structure have zero contribution to the structure's energy dissipations mechanism. The static part of the structure has a significant contribution toward the energy dissipation mechanism of the structure. From NLTHA analysis cumulative energy component, it has been observed that energy dissipation of the applied force is mainly handled by kinetic and Global damping part of the structure. Nonlinear Viscous damping, Nonlinear Hysteretic Damping, and error in the structure have zero contribution toward the energy dissipations mechanism of the structure. Both SPO and NLTHA Force Deformation result for the selected sample hinge types was reasonably similar. This analysis proves that SPO and NLTHA analysis approximation results are reliable despite different analysis procedures and assumptions. IO, LS, and CP performance levels of sample hinges were reasonably the same for both SPO and NLTHA expert for hinge type B88H45 (Auto M3)- which the hinge status pass B to <=C for NLTHA, this result shows the NLTHA analysis applied ground motions can cause the hinge to yield more than SPO used inertial forces. The forces and deformations caused by the applied loading in the structures were generally found in a reasonably similar range for both SPO and NLTHA results. This analysis gave a great insight into when significant actions occurred in our computer model. Most of the movements, strains, deformations or yielding, cracking, and cursing can be seen clearly from the cumulative energy component graph.

8. FUTURE SCOPE AND CONCLUSIONS

This analysis proves that SPO and NLTHA analysis approximation results are reliable despite different analysis procedures and assumptions. IO, LS, and CP performance levels of sample hinges were reasonably the same for both SPO and NLTHA expert for hinge type B88H45 (Auto M3)- which the hing status pass B to <=C for NLTHA, this result shows the NLTHA analysis applied ground motions can cause the hinge to yield

more than SPO applied inertial forces. The forces and deformations caused by the applied loading in the structures were generally found in a reasonably similar range for both SPO and NLTHA results. This analysis gives a great insight into the time when major actions occurred in our computer model. Most of the movements, strains, deformations or yielding, cracking, and cursing can be seen clearly from the cumulative energy component graph. This project has enormous development potential. While the problem focuses on identifying the structural components that have a significant impact on the seismic performance of a future earthquake, this could be extended using PERFORM-3D NONLINEAR design software, eliminating any problematic aspects of designing with ETABS software, and this trend could be used in design consultant offices located throughout the world for safe and economical structure design. The following conclusion were made from the analysis result: -

1. From static pushover analysis cumulative energy component, it has been observed that energy dissipation of the applied force is mainly handled by potential part of the structure.
2. From the analysis, it has been observed that the nonlinear hysteresis damping has a small contribution toward the energy dissipation mechanism of the structure.
3. From the analysis, it has been observed that kinetic, Global Damping, Nonlinear global Damping, and error in the structure have zero contribution toward the energy dissipations mechanism of the structure.
4. From NLTHA analysis cumulative energy component, it has been observed that energy dissipation of the applied force is mainly handled by kinetic and Global damping part of the structure.
5. From the analysis, it has been observed that the static part of the structure has a significant contribution toward the energy dissipation mechanism of the structure.
6. From the analysis, it has been observed that Nonlinear Viscous damping, Nonlinear Hysteretic Damping, and error in the structure have zero contribution toward the energy dissipations mechanism of the structure.
7. Both SPO and NLTHA Force Deformation result for the selected sample hinge types was reasonably similar. This analysis proves that SPO and NLTHA analysis approximation analysis results are reliable even though the analysis procedures and assumptions are different.
8. IO, LS, and CP performance levels of sample hinges were reasonably the same for both SPO and NLTHA expert for hinge type B88H45 (Auto M3)- which the hinge status pass B to <=C for NLTHA, this result shows the NLTHA analysis applied ground motions can cause the hinge to yield more than SPO used inertial forces.
9. In general, the forces and deformations caused by the applied loading in the structures found in a reasonably similar range for both SPO and NLTHA results.
10. This analysis gives a great insight into the time when significant actions occurred in our computer model. Most of the movements, strains, deformations or yielding, cracking, cursing that appeared can be seen clearly from the cumulative energy component graph.

Conflict of interest statement

Authors declare that they do not have any conflict of interest.

REFERENCES

[1] آم وزشمهارتهايورزشي" .كريسدتينا،رود ڤوكورس (راه نمايمربيان)".
ترجمهمحمدتقياقدسي،چاپاول،دانشگاهتبريز No Title," no. August 2005, 1375.

[2] Applied Technology Council, "ATC 40 Seismic Evaluation and Retrofit of Concrete Buildings Redwood City California," Seism. Saf. commisionsion, vol. 1, no. November 1996, p. 334, 1996.

[3] "FEMA 273 DEVELOPMENT -82brady.pdf." .

[4] S. A. Freeman, "Review of the Development of the Capacity Spectrum Method," ISET J. Earthq. Technol., vol. 41, no. 1, p. 113, 2004.

[5] N. K. Shekhar, Y. M. Parulekar, T. Nagender, and J. Chattopadhyay, "Assessment of hysteretic damping in reinforced concrete structures using local hinge characteristics," Bull. Earthq. Eng., vol. 19, no. 1, pp. 135–160, 2021, doi: 10.1007/s10518-020-00968-z.

[6] E. AfsarDizaj and M. M. Kashani, "Nonlinear structural performance and seismic fragility of corroded reinforced concrete structures: modelling guidelines," Eur. J. Environ. Civ. Eng., vol. 0, no. 0, pp. 1–30, 2021, doi: 10.1080/19648189.2021.1896582.

[7] H. AlhajjChehade, D. Dias, M. Sadek, O. Jenck, and F. HageChehade, "Pseudo-static analysis of reinforced earth retaining walls," Acta Geotech., vol. 16, no. 7, pp. 2275–2289, 2021, doi: 10.1007/s11440-021-01148-2.

[8] R. Z. Al-Rousan and A. Sharma, "Integration of FRP sheet as internal reinforcement in reinforced concrete beam-column joints exposed to sulfate damaged," Structures, vol. 31, no. March, pp. 891–908, 2021, doi: 10.1016/j.istruc.2021.02.034.

[9] H. Feng, F. Zhou, H. Ge, H. Zhu, and L. Zhou, "Energy dissipation enhancement through multi-toggle brace damper systems for mitigating dynamic responses of structures," Structures, vol. 33, no. May, pp. 2487–2499, 2021, doi: 10.1016/j.istruc.2021.05.068.

[10] H. Guo, X. Zhou, W. Li, Y. Liu, and D. Yang, "Experimental and numerical study on seismic performance of Q690 high-strength steel plate reinforced joints," Thin-Walled Struct., vol. 161, no. January, p. 107510, 2021, doi: 10.1016/j.tws.2021.107510.

[11] A. Habib, U. Yildirim, and O. Eren, "Seismic Behavior and Damping Efficiency of Reinforced Rubberized Concrete Jacketing," Arab. J. Sci. Eng., vol. 46, no. 5, pp. 4825–4839, 2021, doi: 10.1007/s13369-020-05191-1.

[12] K. Wu, S. Lin, C. Xu, C. Chen, and F. Chen, "Energy dissipation and debonding mechanism of steel and steel fibre reinforced concrete composite beams," Eng. Struct., vol. 226, no. September 2020, p. 111353, 2021, doi: 10.1016/j.engstruct.2020.111353.

[13] X. Zhang and B. Li, "Seismic performance of exterior reinforced concrete beam-column joint with corroded reinforcement," Eng. Struct., vol. 228, no. November, p. 111556, 2021, doi: 10.1016/j.engstruct.2020.111556.